Journal of Hazardous Materials 167 (2009) 52–63

Contents lists available at ScienceDirect

Journal of Hazardous Materials

journal homepage: www.elsevier.com/locate/jhazmat

Modeling and multi-response optimization of pervaporation of organic aqueous solutions using desirability function approach

C. Cojocaru [a], M. Khayet [b,*], G. Zakrzewska-Trznadel [c], A. Jaworska [c]

[a] Department of Environmental Engineering and Management, Faculty of Chemical Engineering, Technical University of Iasi, Iasi, Romania
[b] Department of Applied Physics I, Faculty of Physics, University Complutense of Madrid, Madrid, Spain
[c] Department of Nuclear Methods in Process Engineering, Institute of Nuclear Chemistry and Technology, Warsaw, Poland

ARTICLE INFO

Article history:
Received 2 October 2008
Received in revised form
21 November 2008
Accepted 16 December 2008
Available online 25 December 2008

Keywords:
Water treatment
Optimization
Factorial design of experiments
Pervaporation

ABSTRACT

The factorial design of experiments and desirability function approach has been applied for multi-response optimization in pervaporation separation process. Two organic aqueous solutions were considered as model mixtures, water/acetonitrile and water/ethanol mixtures. Two responses have been employed in multi-response optimization of pervaporation, total permeate flux and organic selectivity. The effects of three experimental factors (feed temperature, initial concentration of organic compound in feed solution, and downstream pressure) on the pervaporation responses have been investigated. The experiments were performed according to a 2^3 full factorial experimental design. The factorial models have been obtained from experimental design and validated statistically by analysis of variance (ANOVA). The spatial representations of the response functions were drawn together with the corresponding contour line plots. Factorial models have been used to develop the overall desirability function. In addition, the overlap contour plots were presented to identify the desirability zone and to determine the optimum point. The optimal operating conditions were found to be, in the case of water/acetonitrile mixture, a feed temperature of 55 °C, an initial concentration of 6.58% and a downstream pressure of 13.99 kPa, while for water/ethanol mixture a feed temperature of 55 °C, an initial concentration of 4.53% and a downstream pressure of 9.57 kPa. Under such optimum conditions it was observed experimentally an improvement of both the total permeate flux and selectivity.

1. Introduction

Nowadays there are increased concerns of the pollution of groundwater and surface water with volatile organic compounds (VOCs). This type of organic contaminants leak from underground storage tanks, municipal and industrial land-fill sites, or are released from industrial and municipal wastewaters [1]. The potential presence of VOCs in natural and drinking waters has led government agencies to oblige to severe regulations and to impose the treatment of VOCs polluted waters as an imperative solution.

According to EC Directive 1999/13/EC (Solvent Emissions Directive), VOCs are functionally defined as organic compounds having at 293.15 K (i.e. 20 °C) a vapor pressure of 0.01 kPa or more, or having a corresponding volatility under particular conditions of use. VOCs may be defined as organic compounds having an initial boiling point lower than or equal to 250 °C at atmospheric pressure (EC Directive 2004/42/EC).

Ethanol and acetonitrile are typical VOCs having boiling points of 65 °C (ethanol) and 82 °C (acetonitrile) and a vapor pressure of 5.85 kPa (ethanol) and 9.54 kPa (acetonitrile) at 20 °C. According to Zhang et al. [2] ethanol is rapidly replacing methyl *tert*-butyl ether (MTBE), which is widely used as fuel oxygenate. Therefore, ethanol releases from spills and leaky underground storage tanks should be anticipated. Such incidents are expected to increase with the growing use of ethanol instead of MTBE as fuels oxygenate. It is worth quoting that ethanol has received little attention as a potential groundwater contaminant and studies concerning removal of ethanol from water are of real interest.

The primary use of acetonitrile compound was as an extracting solvent for unsaturated hydrocarbons (especially butadiene) and in general as solvent for many compounds including fatty acids and oils based on its selective miscibility. Nowadays, acetonitrile is used as a solvent in the production of pharmaceuticals, perfumes, vitamin B, pesticides, and plastics. It is also used in the photographic and textile industry, in the extraction and refining of copper, for the production of lithium batteries, for the extraction of fatty acids from animal and vegetable oils, and in analytical chemistry laboratories [3]. Acetonitrile is toxic to humans and may enter the

* Corresponding author. Tel. +34 91 3945185; fax. +34 91 3945191.
E-mail address: khayetm@fis.ucm.es (M. Khayet).

0304-3894/$ – see front matter © 2008 Elsevier B.V. All rights reserved.
doi:10.1016/j.jhazmat.2008.12.078

Nomenclature

b_0, b_i, b_{ij}	regression coefficients
$\bar{b}$	vector ($u \times 1$) of regression coefficients
C	initial concentration of the organic compound in feed (wt%)
d	individual desirability function
d_J	individual desirability function corresponding to the total permeate flux
d_a	individual desirability function corresponding to selectivity
D	overall desirability function
DF	number of degrees of freedom
F-value	ratio of variances
g	weight factor
h	interval of variation
i, j	subscripts (integer variables)
J	total permeate flux (10^{-4} kg/m^2·s)
J_A	total permeate flux for W/A mixture
$\hat{J}_A$	predictor of total permeate flux for W/A mixture
J_E	total permeate flux for W/E mixture
$\hat{J}_E$	predictor of total permeate flux for W/E mixture
k	subscript (integer variable)
m	number of responses
MS	mean square
n	number of designed variables
N	number of experimental runs
P	downstream pressure (kPa)
R^2	coefficient of multiple determination
R^2_{adj}	adjusted statistic coefficient
SS	sum of squares
T	feed temperature (°C)
w_o	weight fraction of organic compound in feed solution
w_q	weight fraction of water in feed solution
x_1, x_2, x_3	coded levels of factors
$\bar{x}$	vector ($n \times 1$) of coded variables
$\bar{\bar{x}}$	matrix ($N \times u$) of the designed variables levels
y	response
$\hat{y}$	predictor of the response
$\bar{y}$	vector ($n \times 1$) of the response
y_i^-	lower tolerance limit of response
y_i^+	upper tolerance limit of response
z	actual value of designed variable
z^0	center point of designed variable (actual value)
*	superscript indicating optimal values of variables

Greek letters

α	organic selectivity
α_A	organic selectivity for W/A mixture
$\hat{\alpha}_A$	predictor of organic selectivity for W/A mixture
α_E	organic selectivity for W/E mixture
$\hat{\alpha}_E$	predictor of organic selectivity for W/E mixture
Ω	valid region (region of experimentation)
Ω_R	desirability zone (region of interest)

Abbreviations

ANOVA	Analysis of variances
DoE	Design of experiments
FFD	Full factorial design
LTB	Larger-the-best, type of desirability function
MTBE	Methyl *tert*-butyl ether
MLR	Multi-linear regression method
NTB	Nominal-the-best, type of desirability function
PV	Pervaporation
RSM	Response surface methodology
STB	Smaller-the-best, type of desirability function
VOCs	Volatile organic compounds
W/A	Water/acetonitrile mixture
W/E	Water/ethanol mixture

environment through industrial effluent streams, municipal waste treatment plant discharges or spills.

Current technology for the removal of volatile contaminants includes air stripping combined with adsorption onto activated carbon or catalytic oxidation. For higher concentration of VOCs, the cost of disposal/regeneration of the activated carbon becomes quite expensive. Regarding catalytic oxidation, this process is limited only to few systems owing to the problems of catalyst deactivation and poisoning [4]. In the last few decades, membrane separation processes have become more attractive for VOCs removal from aqueous feed solutions [1]. For example, vacuum membrane distillation has been tested for the removal of VOCs from water [5–8]. Furthermore, pervaporation has been proved as a promising separation process for VOCs removal from aqueous feed solution using different types of membranes [5,9–18] and has the potential to be one of the most common techniques in environmental engineering for water purification. The performance of both separation processes, i.e. pervaporation (PV) and vacuum membrane distillation (VMD) has been compared for the separation of chloroform(VOC)/water mixtures [5,19]. In addition to VOCs removal from wastewaters, the most important applications of pervaporation are dehydration of solvents or organic compounds [20–23] and organic/organic separations [24–29].

One of the common experimentation approaches employed by many scientists and engineers in the field of membrane science and technology is One-Variable-At-a-Time (OVAT) methodology, where one of the variables is varied while others are fixed. Such approach depends upon experience, guesswork and intuition for its success. In addition, this type of experimentation methodology demands wide resources to obtain a limited amount of knowledge about the process. OVAT experimentation methodology is often unreliable, inefficient, time consuming, and may yield to a false optimum condition for the investigated process [30]. On the contrary, the statistical tools like design of experiments (DoE) and response surface methodology (RSM) permit the investigation of the process via simultaneous changing of factors' levels using reduced number of experimental runs. Such approach plays an important role in designing and conducting experiments as well as analyzing and interpreting the obtained data. These tools present a collection of mathematical and statistical methods that are applicable for modeling and optimization analysis in which a response or several responses of interest are influenced by various designed variables (factors) [33].

DoE and RSM have been proven to be effective statistical tools for the modeling and optimization of the separation processes in the field of membrane technology [32–35].

The objective of the present study is to optimize the pervaporation operating conditions in order to enhance both membrane selectivity and total permeate flux (PV performance) using desirability function approach.

Table 1
Actual and coded values of independent variables used for experimental design.

Variable	Symbol	Real values of coded levels		
		−1	0 (Center point)	+1
Feed temperature, T (°C)	x_1	30	42.5	55
Initial concentration of organic compound, C (wt%)	x_2	1	5.5	10
Downstream pressure, P (kPa)	x_3	5.34	16	26.66

2. Experimental

2.1. Materials

The PV experiments were carried out using binary aqueous solutions containing ethanol and acetonitrile. Ethanol and acetonitrile chemicals used in all experiments were of analytical grade purchased from POCH Company (Poland). Distilled water has been used in all feed mixtures. The commercial polymeric composite flat-sheet membrane supplied by Sulzer Chemitech GmbH Company with the trade name Pervap^R 4060 has been used in the present study.

2.2. Pervaporation set-up and procedure

Pervaporation experiments were carried out using a laboratory scale pervaporation system detailed elsewhere [36]. The feed chamber of the PV set-up was maintained at a temperature (ranging between 30 and 55 °C) by means of a thermostat. The feed stream, composed of water/acetonitrile (W/A) or water/ethanol (W/E) mixtures with the organic compound concentration ranging from 1 to 10 wt%, was brought in direct contact with the upstream side of the membrane. In all experiments the stirring rate of the feed solution was kept constant at high level to guarantee a turbulent flow pattern. The permeate was collected in liquid nitrogen cold traps and the total permeate fluxes were determined by measuring the weight of the collected liquid in a certain time. The pressure at the downstream side of the membrane was held in the range of 4–27 kPa using a vacuum pump. The effective membrane area of the PV system was 88.22×10^{-4} m^2. The feed and permeate compositions were analyzed by measuring their refractive index by means of a refractometer (RUDOLPH RESEARCH J357). The performance of the PV membrane has been indicated by the total permeate flux (J) and the organic selectivity (α) defined in Eq. (1) [18].

$$\alpha = \frac{(w_o/w_q)_{permeate}}{(w_o/w_q)_{feed}} \quad (1)$$

where w_i and w_j are the weight percentages of components "o" and "q" respectively. The subindex "o" refers to the organic component while "q" refers to water component.

3. Results and discussions

3.1. Pervaporation experimental design

The design of PV experiments combined with RSM is of great interest since such experimental-statistical tools permit to reduce the number of experimental runs and to investigate the interaction effects between the designed variables (factors). Therefore, this methodology was employed for the investigation and optimization of both water/acetonitrile (W/A) and water/ethanol (W/E) pervaporation systems. As stated earlier, the aim of optimization was to improve the performance of PV separations by maximizing the values of two responses, i.e. total permeate flux (J) and selectivity (α). The key variables that affect the responses were selected by performing preliminary tests. These variables are the feed temperature (T), the initial organic compound concentration of the feed stream (C) and the downstream pressure (P). For statistical calculations the actual variables were coded according to Eq. (2).

$$x_i = \frac{z_i - z_i^0}{h_i} \quad \forall i = \overline{1, n} \quad (2)$$

where z denotes the actual value of the designed variable, z^0 is the center point of the designed variable (actual value), h is the interval of variation, x is the coded level of the designed variable (dimensionless value) and n is the number of variables. Thus, each variable has two different coded levels from low (±1) to high (1). A center point was also added to the design for the ease of statistical analysis. Table 1 presents the independent variables with the actual operating range of each variable and corresponding coded levels.

The experimental design adopted in this study consisted of 8 factorial points (full factorial design) and 2 center points (for replication). The full factorial design is a set of experimental runs where each level of the designed variable is investigated at both levels (+1) and (−1) of all the other factors. It is an orthogonal design, which allows the estimation of a factor effect independently of all other effects. Table 2 shows the full factorial design of the PV experiments and the values of two observed responses (J and α) for both mixtures water/acetonitrile and water/ethanol.

Table 2
Full 2^3 factorial design of PV experiments.

Run	Input variables						Responses			
N	Feed temperature		Organic concentration		Downstream pressure		Water/acetonitrile		Water/ethanol	
	T (°C)	Level x_1	C (wt%)	J Level x_2	α P (kPa)	J Level x_3	α J_A 10^{-4} kg/m^{2}s	α_A	J_E 10^{-4} kg/m^{2}s	α_E
1	55	1	10	1	26.66	1	4.082	11.023	0.954	11.414
2	30	−1	10	1	26.66	1	1.025	9.812	0.202	9.696
3	55	1	1	−1	26.66	1	0.372	66.787	0.344	21.639
4	30	−1	1	−1	26.66	1	0.202	15.795	0.131	9.139
5	55	1	10	1	5.34	−1	6.886	11.195	3.309	8.807
6	30	−1	10	1	5.34	−1	2.983	11.327	1.138	4.388
7	55	1	1	−1	5.34	−1	2.392	21.458	2.107	10.714
8	30	−1	1	−1	5.34	−1	0.427	16.393	0.795	3.627
9	42.5	0	5.5	0	16	0	1.453	20.246	0.630	9.058
10	42.5	0	5.5	0	16	0	1.404	20.642	0.664	8.804

3.2. Factorial modeling and analysis

Based on experimental design matrix (Table 2) the factorial models were developed to ascertain the relationship between responses and factor effects. According to this method, a response y is set as a functional relationship of the designed variables (factors) and for a full factorial design the effects of factors may be estimated by linear regression model with interactions:

$$\hat{y} = b_0 + \sum_{i=1}^{n} b_i x_i + \sum_{1\le i<j}^{n} b_{ij} x_i x_j + \sum_{1\le i<j<k}^{n} b_{ijk} x_i x_j x_k \quad (3)$$

where $\hat{y}$ is the predictor of the response, b_0, b_i, and b_{ij} are the regression coefficients and i, j, and k denote the integer positive variables.

In order to ascertain the regression coefficients of the factorial model, Eq. (3), the multi-linear regression (MLR) method was employed. According to this method the least square estimations of the regression coefficients can be written as [31,37–39]:

$$\bar{b} = \left(\bar{\bar{x}}^{\mathrm{T}}\bar{\bar{x}}\right)^{-1}\bar{\bar{x}}^{\mathrm{T}}\bar{y} \quad (4)$$

where $\bar{b}$ is a $(u\times 1)$ vector of regression coefficients, $\bar{\bar{x}}$ is a $(N\times u)$ matrix of the independent variables levels, $\bar{y}$ is a $(N\times 1)$ vector of the response (experimental values), N is the number of experimental runs and u is the number of regression coefficients that appear in factorial model. According to the experimental design presented in Table 2, the interaction models were established for each case and for each response (J and α), which may be written in terms of coded factors as follows:

- For water/acetonitrile (W/A) mixture:

$$\hat{J}_{\mathrm{A}} = 2.296 + 1.137x_1 + 1.448x_2 - 0.876x_3 + 0.603x_1x_2 - 0.33x_1x_3 - 0.315x_2x_3 + 0.119x_1x_2x_3 \quad (5)$$

$$\hat{\alpha}_{\mathrm{A}} = 20.473 + 7.142x_1 - 9.634x_2 + 5.38x_3 - 6.872x_1x_2 + 5.908x_1x_3 - 5.802x_2x_3 + 5.573x_1x_2x_3 \quad (6)$$

- For water/ethanol (W/E) mixture:

$$\hat{J}_{\mathrm{E}} = 1.1225 + 0.5560x_1 + 0.2783x_2 - 0.7148x_3 + 0.1748x_1x_2 - 0.3148x_1x_3 - 0.1080x_2x_3 - 0.04x_1x_2x_3 \quad (7)$$

$$\hat{\alpha}_{\mathrm{E}} = 9.9279 + 3.2154x_1 - 1.3519x_2 + 3.0439x_3 - 1.6814x_1x_2 - 1.0654x_2x_3 - 1.0144x_1x_2x_3 \quad (8)$$

Table 3
ANOVA table for factorial models.

Source	DF[a]	SS[b]	MS[c]	F-value	R^2	R^2_{adj}
Water/acetonitrile mixture, response: (J_A)						
Model	7	37.633	5.376	7.137	0.962	0.827
Residual	2	1.507	0.753			
Total	9	39.14				
Water/acetonitrile mixture, response: (α_A)						
Model	7	2557.09	365.3	9063.9	0.9999	0.9998
Residual	2	0.081	0.04			
Total	9	2557.17				
Water/ethanol mixture, response: (J_E)						
Model	7	8.219	1.174	5.044	0.946	0.759
Residual	2	0.466	0.233			
Total	9	8.685				
Water/ethanol mixture, response: (α_E)						
Model	7	210.981	30.14	20.513	0.986	0.938
Residual	2	2.939	1.469			
Total	9	213.92				

[a] DF: degrees of freedom.
[b] SS: sum of squares.
[c] MS: mean square.

The design variables that appear in regression Eqs. (5)–(8) are subjected to the following constraints:

$$x_i \in \Omega;\ \Omega = \{x_i | -1 \le x_i \le +1\};\quad \forall i = \overline{1,3}$$

where x_1, x_2 and x_3 denote the coded levels of the designed variables (factors) and Ω is the valid region (region of experimentation). It should be mentioned that all regression coefficients retained in Eqs. (5)–(8) are the significant ones, i.e. the significance of each individual regression coefficient has been tested by means of Student's t-test [37].

The analysis of variance (ANOVA) was used to verify the statistical significance of the interaction models. The F-value, which is a measure of the variance of the data to the mean, was determined based on the ratio of mean square of group variance due to the error [31]. The greater is the F-value from unity, the more certain is that the designed variables (factors) adequately explain the variation in the mean of the data. The ANOVA results are presented in Table 3 for all interaction models. The ANOVA table summarizes the sum of squares of residuals and regressions together with the corresponding degrees of freedom, F-value and ANOVA coefficients (i.e. coefficients of multiple determination R^2 and adjusted R^2_{adj} statistic). The mathematical expressions used for the calculation of the ANOVA estimators (i.e. SS, MS, F-value, R^2, R^2_{adj}) are widely presented in the literature concerning the response surface methodology [31,37]. According to ANOVA table, the F-value is quite

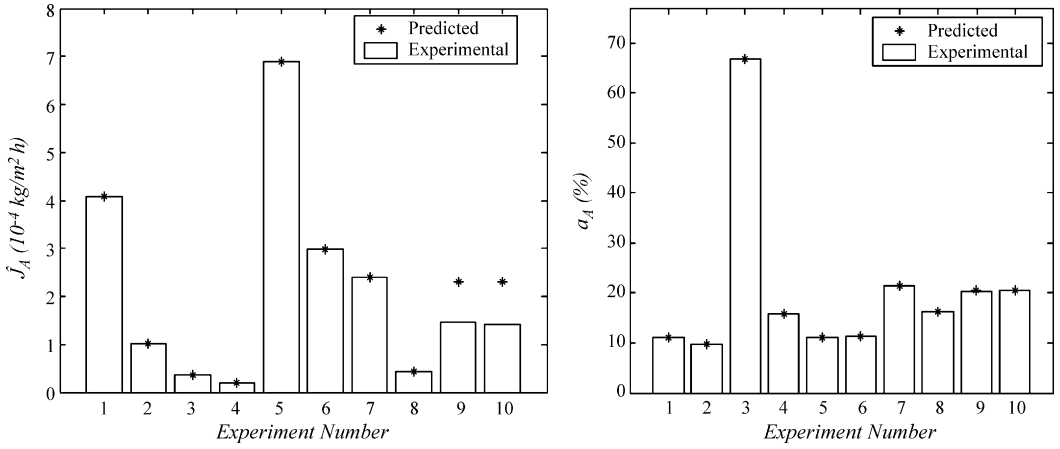

Fig. 1. Experimental data versus predicted values by factorial models, water/acetonitrile PV mixture.

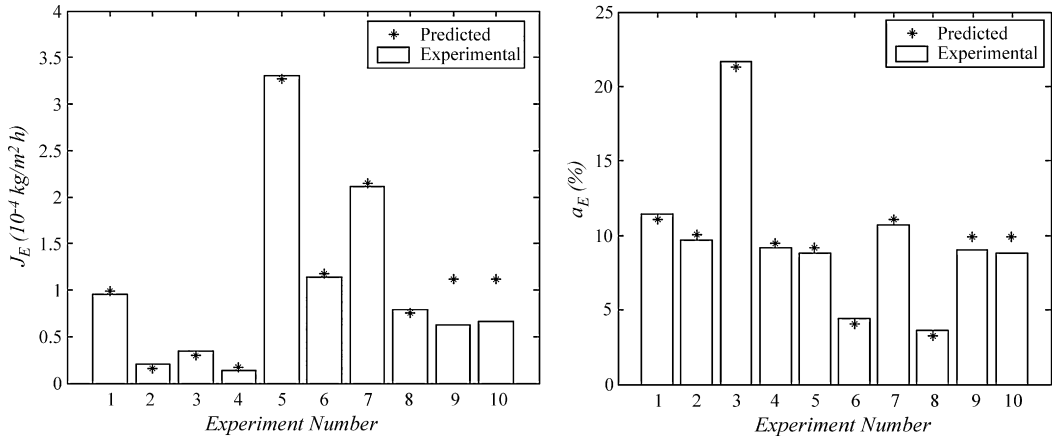

Fig. 2. Experimental data versus predicted values by factorial models, water/ethanol PV mixture.

high and the R^2 values are close to 1, which is acceptable. In addition, the predicted R^2 is in agreement with the adjusted coefficients of determination, R^2_{adj}. All these statistical estimators reveal that interaction factorial models are statistically accepted for the prediction of the two responses in the considered range of experimentation (valid region).

The comparison of the predicted and experimental responses is shown in Figs. 1 and 2 against the observation order (i.e. the number of experimental run N). The results reported in Figs. 1 and 2 show a goodness-of-fit between interaction factorial models and the corresponding experimental set of data. As can be observed in Fig. 1 (W/A mixture), for both models the predicted data are identical to the experimental ones for the orthogonal points (1–8). In the center points (9–10) the discrepancy between the predicted and the experimental data is visible only for the total permeate flux model. This means that the regression equation for the permeate flux J_A does not describe very well the response in the center point. This behavior can be attributed to the orthogonal property of the factorial design. However, based on the ANOVA statistical test the overall prediction is considered satisfactory. For the selectivity the interaction model predicts very well the response in all points including the center points. According to Fig. 2 (W/E mixture) the goodness-

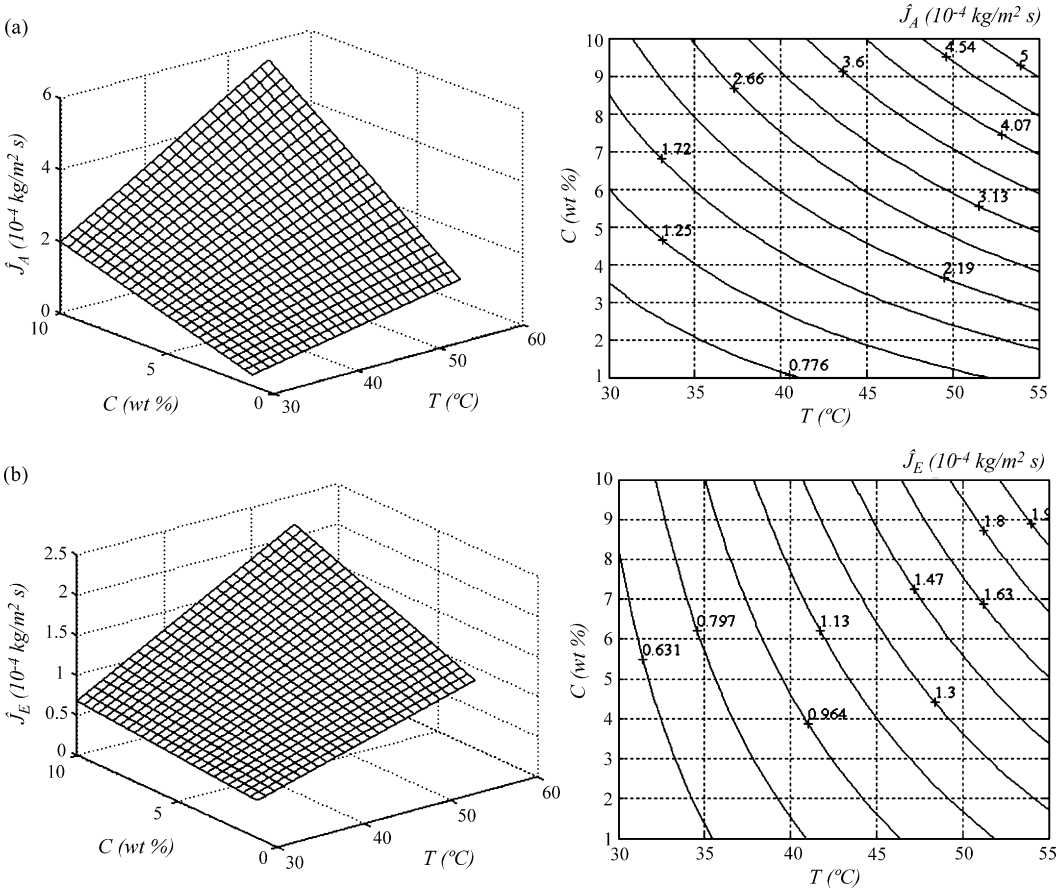

Fig. 3. Response surface plots and contour plots showing the effect of organic compound concentration (wt%), feed temperature (°C) and their mutual interaction on the total permeate flux (J) at P = 16 kPa. (a) Water/acetonitrile PV mixture. (b) Water/ethanol PV mixture.

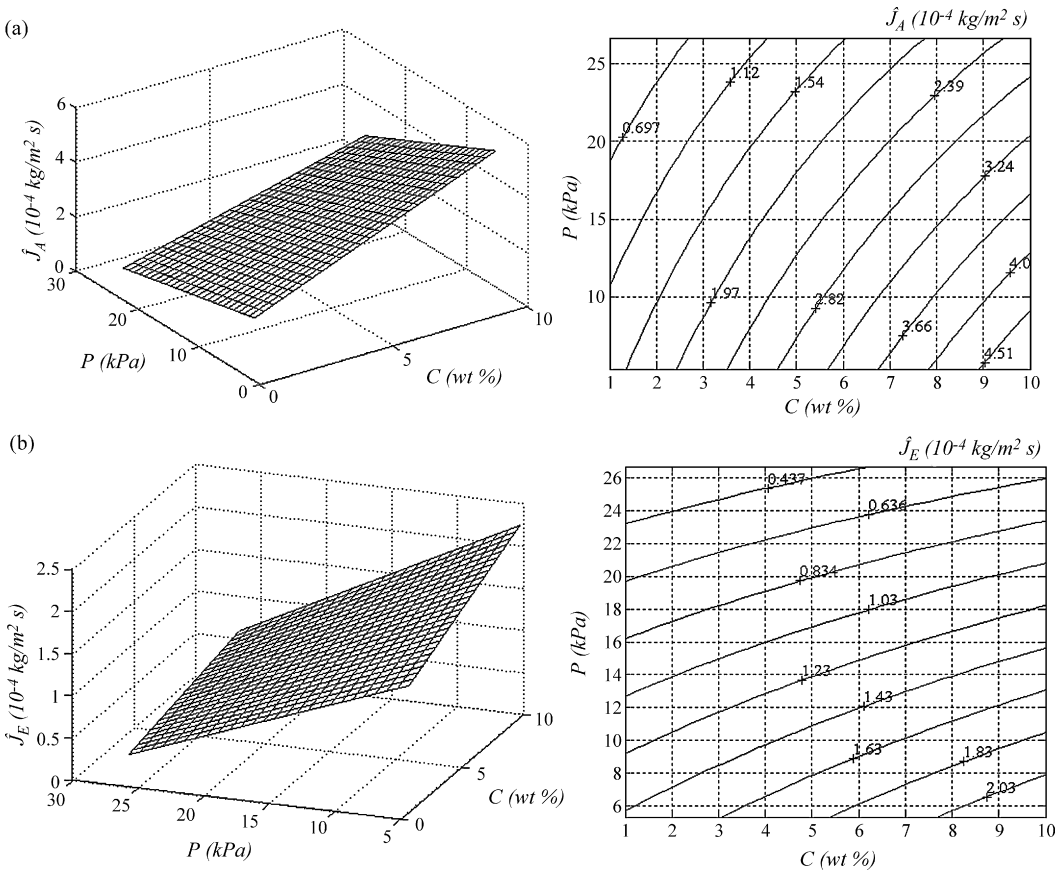

Fig. 4. Response surface plots and contour plots showing the effect of organic compound concentration (wt%), downstream pressure (kPa) and their mutual interaction on the total permeate flux (J) at T = 42.5 °C. (a) Water/acetonitrile PV mixture. (b) Water/ethanol PV mixture.

of–fit is the best for the orthogonal points while for the central points the residual error is slightly larger.

It should be noted here that the factorial models in terms of the coded variables, i.e. Eqs. (5)–(8), are more useful for optimization since the valid region for each individual coded variable is in fact the same interval of variation, i.e. from −1 to +1. For graphical representation and analysis of response surface, the factorial models in terms of coded variables are converted to empirical models in terms of actual variables. The empirical coefficients for regression equations in terms of actual factors have been computed by means of substitution technique. Thus, the factorial models converted in terms of actual variables may be written for each case as follows:

- For water/acetonitrile mixture:

$$\hat{J}_A = -2.52 + 0.089T + 0.106C + 0.105P + 7.56 \times 10^{-3}TC - 3.565 \times 10^{-3}TP - 0.015CP + 1.98 \times 10^{-4}TCP \quad (9)$$

$$\hat{\alpha}_A = 25.6 - 0.284T - 1.333C - 2.887P + 0.027TC + 0.095TP + 0.274CP - 9.294 \times 10^{-3}TCP \quad (10)$$

- For water/ethanol mixture:

$$\hat{J}_E = -1.113 + 0.065T - 0.034C + 0.046P + 3.108 \times 10^{-3}TC - 2.362 \times 10^{-3}TP - 2.251 \times 10^{-3}CP \quad (11)$$

$$\hat{\alpha}_E = -6.535 + 0.273T + 0.175C + 0.012P - 2.824 \times 10^{-3}TC + 9.304 \times 10^{-3}\,TP + 0.05CP - 1.692 \times 10^{-3}TCP \quad (12)$$

where the experimental factors are subjected to the following constraints (experimental region):

$$30 \le T \le 55(^\circ\text{C}); \quad 1 \le C \le 10(\text{wt\%}); \quad 5.34 \le P \le 26.66\,(\text{kPa})$$

The MATLAB program was employed to visualize the three dimensional (3D) response surfaces and the corresponding contour plots of the total permeate flux, J (Figs. 3–5) and selectivity α (Figs. 6–8) with the independent designed variables. The response plots for both mixtures are presented with the vertical axes showing the responses and each of the two horizontal axes representing two designed variables keeping the third variable at constant level (central level). For a first-order interaction model, when the interaction effect between factors is negligible then the response surface is a plane and the corresponding contour plot contains parallel straight lines. If the interaction effect is significant then the plane becomes “twisted”. This twisting of the response surface results in curved contour lines of constant response in the plane of the designed variables. Thus, the interaction effect is a form of curvature in the underlining factorial model for the experiment [31].

The response surface plots and contour plots of the total permeate flux are presented in Figs. 3–5 for both PV systems (W/A and W/E). These plots reveal that the increase of feed temperature and initial organic compound concentration lead to an increase of the total permeate flux. In contrast, the increment of the downstream pressure decreases this response.

In the case of W/A mixture, the main effect of the initial organic compound concentration is the highest one, followed by that of feed temperature. The main effect of the downstream pressure is

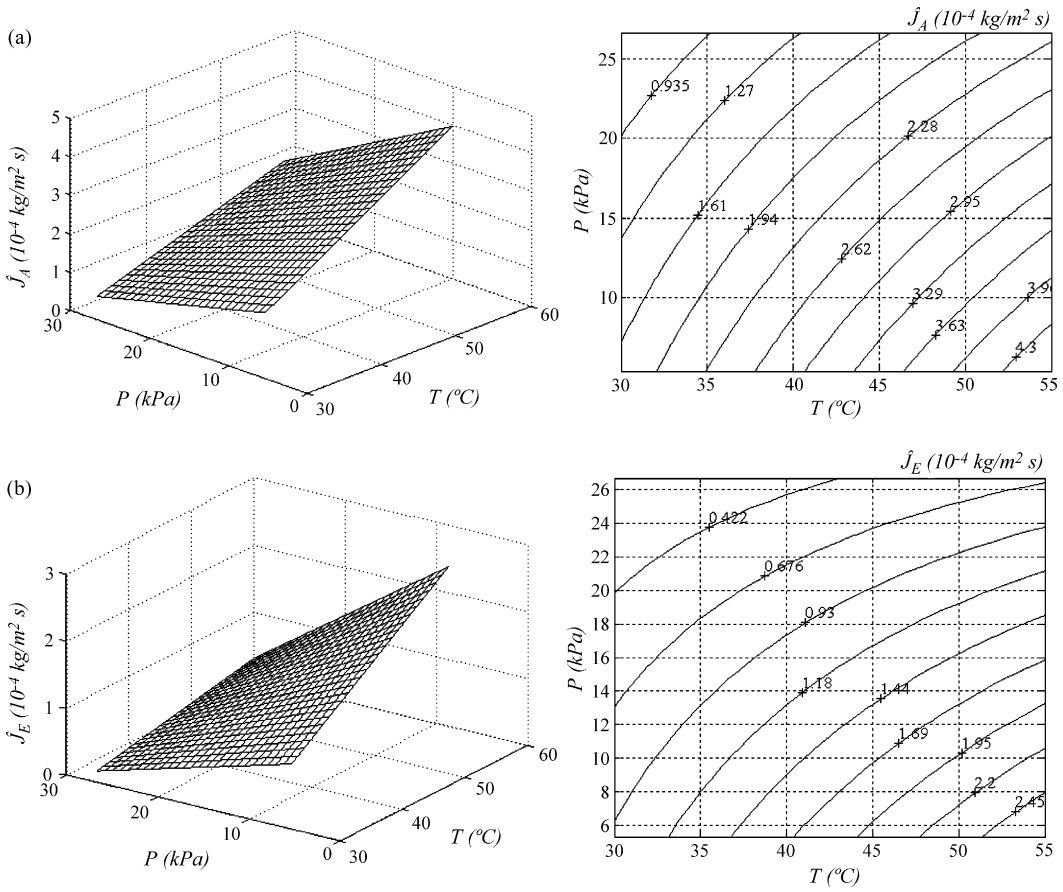

Fig. 5. Response surface plots and contour plots showing the effect of downstream pressure (kPa), feed temperature (°C) and their mutual interaction on the total permeate flux (J) at C = 5.5%. (a) Water/acetonitrile PV mixture. (b) Water/ethanol PV mixture.

smaller in this case than that of feed temperature. On the contrary, for W/E mixture, the main effect of the downstream pressure on the total permeate flux is higher than that of the feed temperature. For this last mixture (W/E) the main effect of the organic compound concentration has the smallest impact upon the total permeate flux.

As far as the interaction effects between the design variables (factors) are concerned, it was observed the following. In the case of W/A mixture, the strongest interaction effect appears between the feed temperature and the initial organic compound concentration (Fig. 3a). According to Fig. 3a, the effect of the feed temperature is more significant at higher organic compound concentrations and the effect of the initial organic compound concentration is greater at higher feed temperatures. As it is shown in Fig. 4a, the interaction effect between the downstream pressure and the initial organic compound concentration is the reduced one. Also, Fig. 5a shows a moderate interaction effect between the downstream pressure and the feed temperature indicating that the effect of the feed temperature is greater at lower downstream pressures.

For W/E mixture, the interaction effect between the feed temperature and the initial organic compound concentration is not so strong as it is for W/A mixture, but it should be taken into account since the curved contour lines are apparent as can be observed in Fig. 3b. In this case, the feed temperature seems to be more significant at high initial organic concentration and vice versa. From Fig. 4b it is clear that the interaction effect between the downstream pressure and the initial organic compound concentration is not significant. The interaction effect between the downstream pressure and the feed temperature (Fig. 5b) is the most relevant interaction effect for W/E mixture. Thus, the influence of the feed temperature is more significant at lower values of the downstream pressure while the influence of the downstream pressure is more relevant for higher feed temperatures. Regarding the interaction between all factors (i.e. T–C–P) and its influence on the total permeate flux it should be mentioned that such interaction is greater in the case of W/A mixture compared to W/E mixture.

In Figs. 6–8 the graphical response surface analysis indicates that the increase of both the feed temperature and the downstream pressure conducts to an enhancement of the organic selectivity. In contrast, the increase of the initial organic compound concentration decreases this response for both mixtures.

In the case of W/A mixture, the most important main effect upon selectivity is attributed to the initial organic compound concentration, followed by the main effect of the feed temperature. Regarding the influence of the downstream pressure, the main effect of this factor is lower than the effect of the feed temperature.

In the case of W/E mixture, the main effect of the initial organic compound concentration is much smaller than the main effects of the feed temperature and the downstream pressure.

Concerning the interactions between the designed variables and their mutual effects upon the organic selectivity, in the case of W/A mixture, the interaction effects between the designed factors are significant and are similar in magnitude for all interactions, i.e. T–C, T–P and C–P. For example in Fig. 6a, the interaction effect between the feed temperature and the organic compound concentration is shown. According to this interaction the influence of the feed temperature is more important at low organic concentration values, while the effect of the organic concentration is more sig-

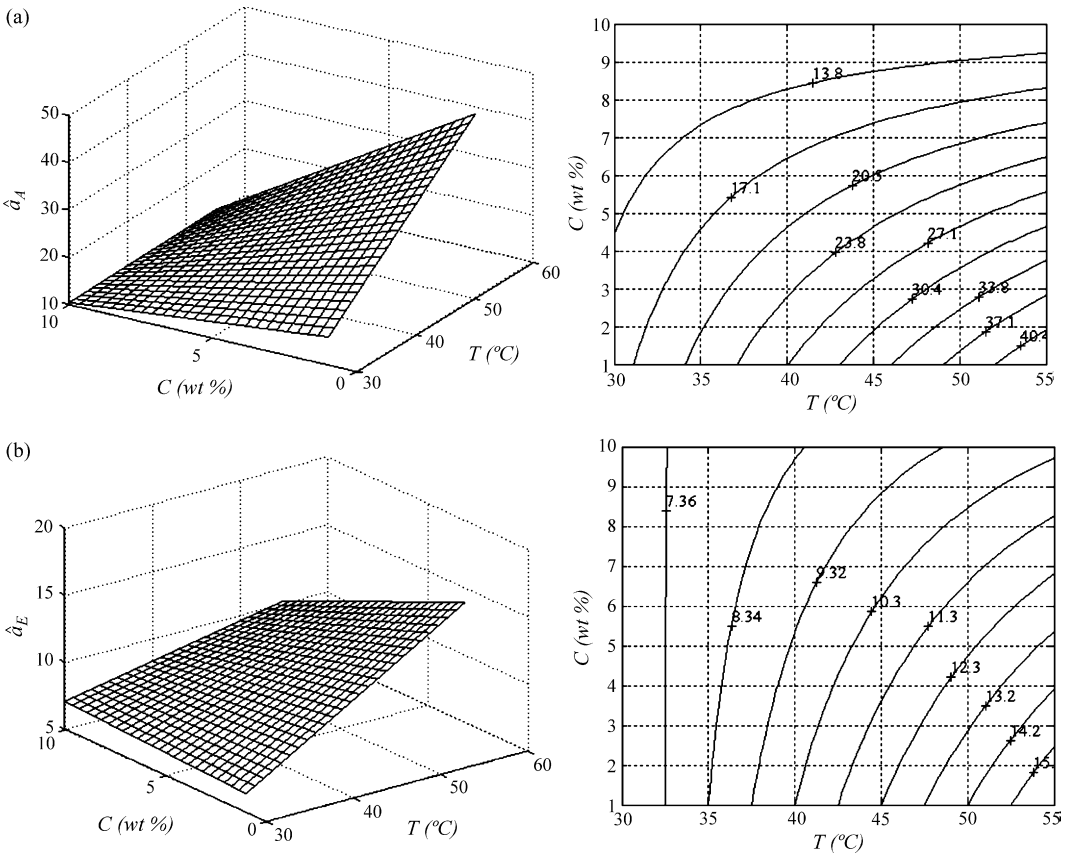

Fig. 6. Response surface plots and contour plots showing the effect of organic compound concentration (wt%), feed temperature (°C) and their mutual interaction on the organic selectivity at $P = 16$ kPa. (a) Water/acetonitrile PV mixture. (b) Water/ethanol PV mixture.

nificant at high temperature. Fig. 7a reveals the interaction effect between *P* and *C* factors. The influence of the downstream pressure upon selectivity is more considerable for low values of organic compound concentration. In contrast, the effects of the initial organic compound concentration are significant at high values of the downstream pressure. Interaction effects appear also between the factors *T* and *P* as can be seen in Fig. 8a. The effect of the downstream pressure is significant at high levels of feed temperature. For low values of feed temperature the influence of the downstream pressure is negligible. Moreover, the effect of the feed temperature is considerable at high levels of the downstream pressure, while at the low values of the downstream pressure the influence of the feed temperature is reduced.

In the case of W/E mixture the interaction effect between the feed temperature and the organic compound concentration (Fig. 6b) is more pronounced than the interaction between the downstream pressure and the organic compound concentration as can be seen in Fig. 7b. Fig. 6b reveals that the effect of the feed temperature upon the organic selectivity became more important at lower values of organic concentration, whereas the influence of the organic compound concentration became more significant at higher values of feed temperature. According to the interaction effects shown in Fig. 7b, the effect of the downstream pressure on organic selectivity is greater at lower organic concentration values. Furthermore, the decrease of the organic selectivity with the increase of the organic concentration is observed at higher values of the downstream pressure. Fig. 8b indicates that there is no interaction between the feed temperature and the downstream pressure for W/E mixture.

Concerning the interaction effect between all factors (i.e. *T*–*C*–*P*) upon the organic selectivity, it must be mentioned that it is much greater in the case of W/A mixture than for W/E mixture. The response surface analysis of both mixtures reveals that the responses (*J* and α) are much higher for W/A mixture.

3.3. Response surface optimization using desirability function approach

The response surface optimization discussed in this section involves the analysis of two pervaporation responses, namely, the total permeate flux (*J*) and the organic selectivity (α). These two responses are of practical importance, since as usual they are in conflict with each other. For example, the results listed in Table 2 reveal that the higher values of the total permeate flux do not involve at the same time the higher values of the organic selectivity. Therefore it is necessary to find out the optimal point as a compromise between the higher total permeate flux and selectivity. A useful approach to solve a multiple response optimization problem is to use the simultaneous optimization technique proposed by Derringer and Suich [40]. This computation procedure involves the desirability functions. According to this approach, each predictor of response $\hat{y}_i(\bar{x})$ is firstly converted to an individual desirability function (d_i) that varies over the range $0 \leq d_i \leq 1$. There are three forms of the desirability function depending on response's characteristic [40–43]: (1) the-larger-the-best (LTB-type) – for an objective function to be maximized; (2) the-smaller-the-best (STB-type) – for an objective to be minimized; and (3) the-nominal-the-best (NTB-type) – for an objective function required to achieve a particular target.

In our specific case, both responses (i.e. total permeate flux and selectivity) should be maximized. Therefore, the corresponding individual desirability functions are the-larger-the-best (LTB-type). The individual desirability function LTB-type can be written in a

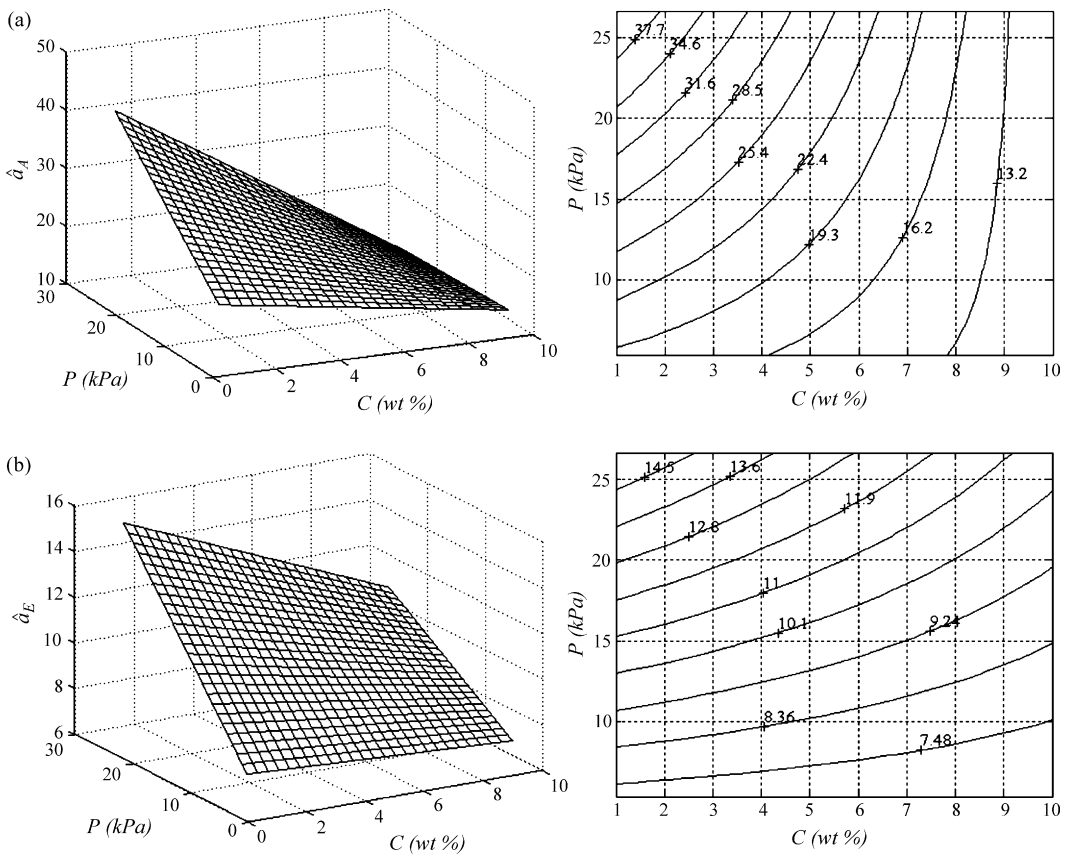

Fig. 7. Response surface plots and contour plots showing the effect of organic compound concentration (wt%), downstream pressure (kPa) and their mutual interaction on the organic selectivity at $T = 42.5\,^{\circ}$C. (a) Water/acetonitrile PV mixture. (b) Water/ethanol PV mixture.

general form as:

$$d_i(\hat{y}_i(\bar{x})) = \begin{cases} 0, & \text{if } \hat{y}_i(\bar{x}) \le y_i^- \\ \left(\dfrac{\hat{y}_i(\bar{x}) - y_i^-}{y_i^+ - y_i^-}\right)^g, & \text{if } y_i^- \le \hat{y}_i(\bar{x}) \le y_i^+ \\ 1, & \text{if } \hat{y}_i(\bar{x}) > y_i^+ \end{cases} \quad (13)$$

where y_i^- presents the lower tolerance limit of the response, the y_i^+ presents the upper tolerance limit of the response and the superindex g represents the weight factor.

In a multi-response situation, the ideal case is when each individual desirability function is unity (=1). In this case, the overall desirability D is also equal to 1. In a real situation, we are interested in maximizing the overall desirability function $D(\bar{x})$, which may be computed as geometric mean of the individual desirability functions $d_i\left(\hat{y}_i(\bar{x})\right)$ as shown in the following equation [40–43]:

$$D(\bar{x}) = \left[d_1\left(\hat{y}_1(\bar{x})\right) \times d_2\left(\hat{y}_2(\bar{x})\right) \times \cdots \times d_m\left(\hat{y}_m(\bar{x})\right)\right]^{1/m} \quad (14)$$

where m denotes the number of responses. Note that if an individual desirability function is completely undesirable, i.e. $d_i\left(\hat{y}_i(\bar{x})\right) = 0$, then the overall desirability value is zero.

The desirability function approach applied in the present PV process joins both responses (i.e. total permeate flux and selectivity) in one overall desirability function that may be written in this case as:

$$D(\bar{x}) = \sqrt{d_J\left(\hat{J}(\bar{x})\right) \times d_\alpha\left(\hat{\alpha}(\bar{x})\right)} \quad (15)$$

where D denotes the overall desirability function, $\bar{x}$ is the vector of the designed variables (coded values), i.e. $\bar{x} = [x_1\, x_2\, x_3]^T$, d_J is the individual desirability function corresponding to the first response (i.e. total permeate flux), d_α is the individual desirability function corresponding to selectivity (second response), $\hat{J}$ is the predictor of the total permeate flux given by the regression Eqs. (5) and (7), $\hat{\alpha}$ is the predictor of the organic selectivity given by the regression Eqs. (6) and (8). Each individual desirability function has been computed by means of Eq. (13) adopting a weight factor $g = 0.5$. In order to ensure a desirability solution, the setting of lower and upper tolerance limits is of great importance in evaluating the individual desirability functions. First, these limits were set by a detailed inspection of the response data in Table 2. For example in the case of W/A mixture, the maximal value of the total permeate flux is 6.886 kg/m^2.s followed by the value 4.082 kg/m^2.s (4.082 is the second highest value of the total permeate flux shown in Table 2). Therefore, the interval (i.e. lower and upper limits) selected to ensure a desirability value of this response is $4.082 \le \hat{J}_A(\bar{x}) \le 6.886$. The lower and upper tolerance limits of the other responses were deduced in a similar way to ensure the desirability solutions. Thus, the desirability domains of responses may be written in first phase as:

- For water/acetonitrile (W/A) mixture:

$$\begin{aligned} &4.082 \le \hat{J}_A(\bar{x}) \le 6.886 \\ &21.458 \le \hat{\alpha}_A(\bar{x}) \le 66.787 \end{aligned} \quad (16)$$

- For water/ethanol (W/E) mixture:

$$\begin{aligned} &2.107 \le \hat{J}_E(\bar{x}) \le 3.309 \\ &11.414 \le \hat{\alpha}_E(\bar{x}) \le 21.639 \end{aligned} \quad (17)$$

The desirability intervals presented as constraint conditions (16) and (17) were refined in the second phase by plotting the overlap contour lines for each response (Figs. 9 and 10). For example, Fig. 9 shows the overlap plot of both responses (J and α) in the coor-

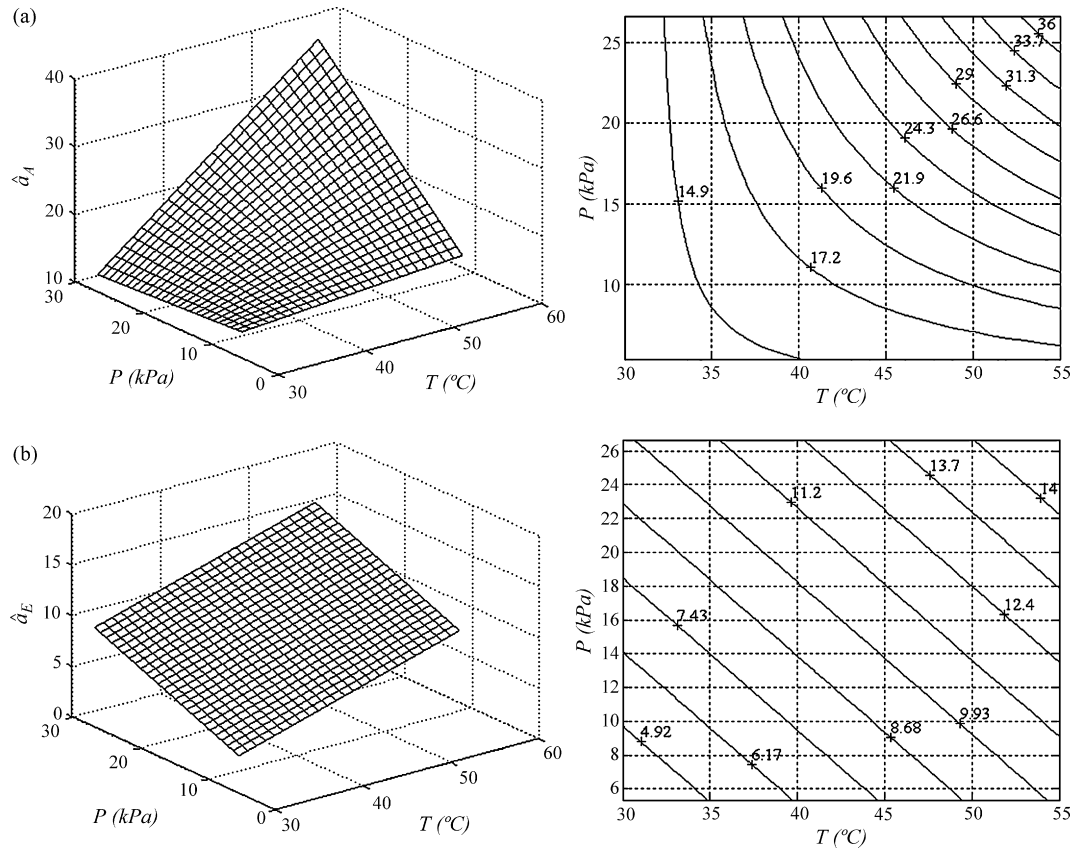

Fig. 8. Response surface plots and contour plots showing the effect of downstream pressure (kPa), feed temperature (°C) and their mutual interaction on the organic selectivity at $C = 5.5\%$. (a) Water/acetonitrile PV mixture. (b) Water/ethanol PV mixture.

dinates P–C by maintaining the third variable (feed temperature) at a constant level, i.e. $T = 53\,^{\circ}C$. By a strict inspection of the contour lines plotted in Fig. 9, one can see that there are no conditions for P and C factors to satisfy the desirability defined in constraints (16) and (17). Furthermore, at lower values of the feed temperature ($T < 53\,^{\circ}C$) such conditions cannot be detected. The desirability zone, known also as region of interest $\Omega_R \subset \Omega$, is visible at higher values of feed temperature (i.e. $T > 53\,^{\circ}C$). The desirability zone, which satisfies the restrictions (16) and (17), is indicated in yellow color for the highest feed temperature value ($T = 55\,^{\circ}C$). Therefore, the optimal points are located in the desirability zones (yellow zones in Fig. 10) and to determine their coordinates and to ensure a high desirability, the constraints (16) and (17) must be refined. According to the overlap plots presented in Fig. 10, the desirability zone (region of interest, $\Omega_R \subset \Omega$) is given by the following refined constraints.

- For water/acetonitrile (W/A) mixture:

$$4.082 \le \hat{J}_A(x) \le 4.20$$
$$21.458 \le \hat{\alpha}_A(\bar{x}) \le 24.00 \qquad (18)$$

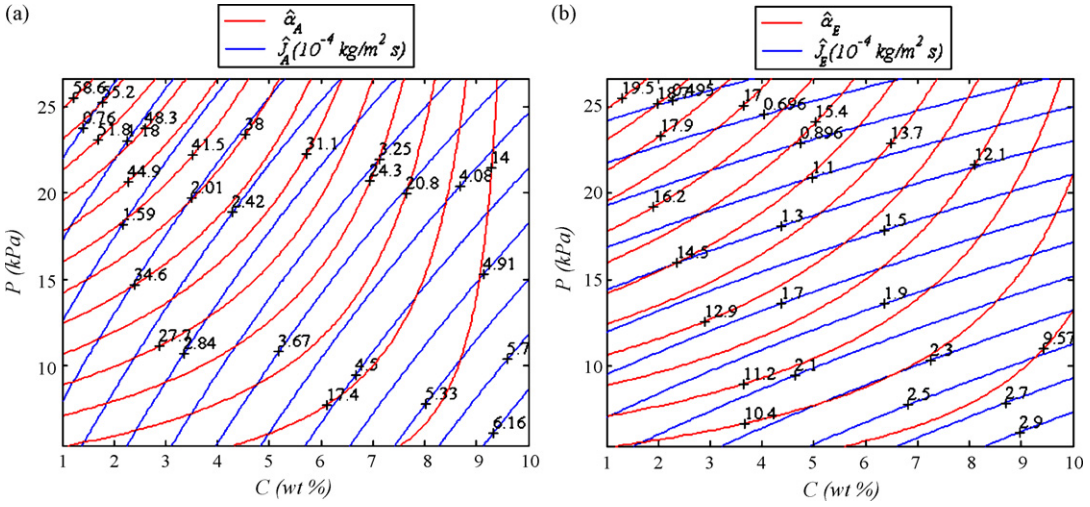

Fig. 9. Contour response surfaces overlap plots for $T = 53\,^{\circ}C$. (a) Water/acetonitrile mixture. (b) Water/ethanol mixture.

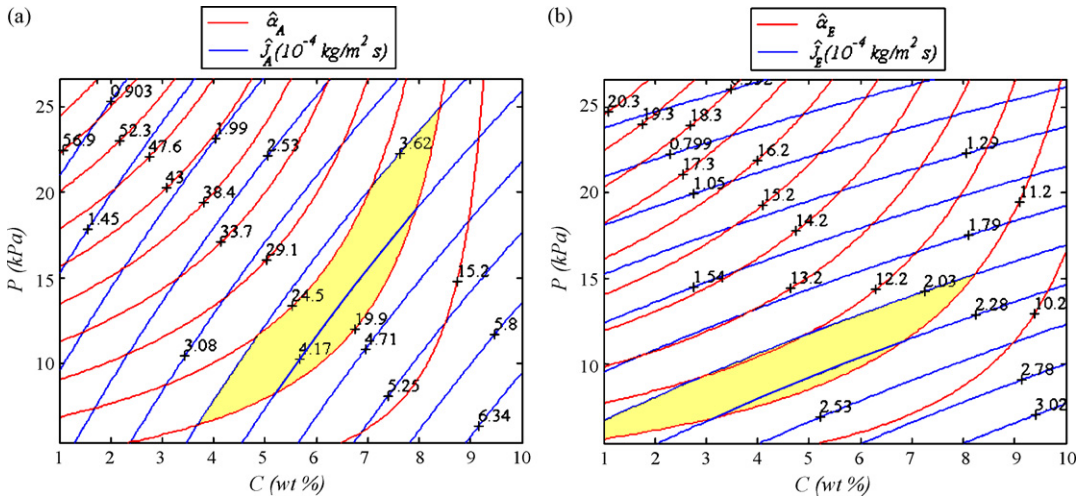

Fig. 10. Contour response surfaces overlap plots for $T = 55\,^{\circ}$C. (a) Water/acetonitrile mixture. (b) Water/ethanol mixture.

Table 4
Optimal conditions for pervaporation of water/acetonitrile and water/ethanol mixtures.

Factors & responses			Water/acetonitrile	Water/ethanol
Factors	Feed temperature	${}^*x_1$ (coded value)	1	1
		${}^*T$ (°C)	55	55
	Initial feed organic concentration	${}^*x_2$ (coded value)	0.2405	−0.2154
		${}^*C$ (wt%)	6.58	4.53
	Downstream pressure	${}^*x_3$ (coded value)	−0.1894	−0.6036
		${}^*P$ (kPa)	13.98	9.57
Responses	Total permeate flux	$\hat{J}({}^*x_1, {}^*x_2, {}^*x_3)$	4.164	2.188
	Organic selectivity	$\hat{\alpha}({}^*x_1, {}^*x_2, {}^*x_3)$	22.026	11.689
	Desirability function	$D(\hat{J}, \hat{\alpha})$	0.6276	0.6299

- For water/ethanol (W/E) mixture:

$$2.107 \le \hat{J}_E(x) \le 2.30$$
$$11.414 \le \hat{\alpha}_E(\bar{x}) \le 12.15 \quad (19)$$

The desirability optimal solution in the case of W/A mixture must satisfy simultaneously both constraints upon $\hat{J}_A(\bar{x})$ and $\hat{\alpha}_A(\bar{x})$ defined by the inequalities (18). Similarly, the desirability optimal solution in the case of W/E mixture must satisfy both restrictions indicated in Eq. (19). To find out the optimal solution localized in the desirability zone $\Omega_R \subset \Omega$, the overall desirability function approach was employed and the constrained optimization problem was written as:

$$\max_{\bar{x} \in \Omega_R} D(\bar{x}) = \max_{\bar{x} \in \Omega_R} \left(\sqrt{d_J\left(\hat{J}(\bar{x})\right) \times d_\alpha\left(\hat{\alpha}(\bar{x})\right)} \right) \quad (20)$$

The optimization of the overall desirability function D involves the maximization of both responses (J and α). The optimization computations have been performed by Monte Carlo stochastic simulation method [38]. According to this method 10^4 points were scattered randomly inside the region of interest. Each point corresponds to a combination of the designed variables. The responses, flux, selectivity and desirability function were computed for all 10^4 points. The stochastic simulations were performed by multistage approach using a zoom-in technique in order to identify the optimal region more accurately. The stochastic simulations and zoom-in technique lead to determine the final Pareto optimal region. The sensitivity analysis employed has revealed that the changes of factors and the response functions along the Pareto front are not significant. Therefore, the optimal solutions were computed as mean values of the factors from the Pareto optimal sets.

The results of the developed optimization are presented in Table 4 for both pervaporation mixtures, i.e. water/acetonitrile (W/A) and water/ethanol (W/E). The optimal feed temperature of both cases is $T = 55\,^{\circ}$C. The optimal solute concentration is 6.58 wt% for W/A mixture and 4.53 wt% for W/E mixture. The optimal downstream pressure is 13.98 kPa for W/A mixture and 9.57 kPa for W/E mixture. Under the optimal conditions of both mixtures, the values of the responses are the following. For W/A mixture, the total permeate flux $\hat{J}_A = 4.164 \times 10^{-4}$ kg/m^2 s and the organic selectivity is $\hat{\alpha}_A = 22.026\%$. This combination is the best one compared with the data presented in Table 2. For W/E mixture, the total permeate flux is $\hat{J}_E = 2.188 \times 10^{-4}$ kg/m^2 s and the organic selectivity is $\hat{\alpha}_E = 11.689\%$. Again this combination is the best one compared to the other combinations presented in Table 2 for ethanol–water mixture.

To check experimentally the obtained optimal points, the confirmation runs were carried out applying the PV operational conditions reported above. The values of the experimental responses are the following.

- For W/A mixture, $J_A = 3.51 \times 10^{-4}$ kg/m^2 s and $\alpha_A = 30.6\%$.
- For W/E mixture, $J_E = 2.02 \times 10^{-4}$ kg/m^2 s and $\alpha_E = 13.14\%$.

As can be seen, the experimental values of the output responses (J and α) obtained considering the obtained optimal conditions represent the best (maximal) values throughout the all conducted experimental tests summarized in Table 2. Therefore, by applying the desirability function approach maximal output responses have been predicted and confirmed experimentally.

4. Conclusions

In this study an optimization approach incorporating the factorial modeling and analysis as well as the desirability function

approach was applied for multi-response optimization of pervaporation process. The multi-response optimization was applied in order to solve a conflict relationship between the two pervaporation responses, the total permeate flux and selectivity, guaranteeing the high values of both. A full factorial design involving a reduced number of experimental runs to localize the optimum PV conditions was followed for water/acetonitrile and water/ethanol mixtures. By factorial modeling and analysis, the main and interaction effects of the factors were identified and discussed. The overlap plot procedure was used to identify the desirability zone and the proper limits. The optimal operational conditions of pervaporation process were ascertained by factorial modeling and desirability function approach. These optimal conditions are: (1) for water/acetonitrile (W/A) mixture: $T = 55\,^{\circ}C$, $C = 6.58$ wt% and $P = 13.98$ kPa and (2) for water/ethanol (W/E) mixture: $T = 55\,^{\circ}C$, $C = 4.53$ wt% and $P = 9.57$ kPa. Under these conditions the high values of both responses, i.e. total permeate flux and selectivity, have been established simultaneously.

Acknowledgements

The present work was performed at the Department of Nuclear Methods and Process Engineering, Institute of Nuclear Chemistry and Technology Warsaw and was financially supported by FP6 European Funds under Marie Curie project: AMERAC no. MTKD-CT-2004-509226. The authors acknowledge this financial support.

References

[1] F.A. Banat, J. Simandl, Removal of benzene traces from contaminated water by vacuum membrane distillation, Chem. Eng. Sci. 51 (1996) 1257–1265.
[2] Y. Zhang, I.A. Khan, X.H. Chen, F. Roy, Spalding, transport and degradation of ethanol in groundwater, J. Contam. Hydrol. 82 (2006) 183–194.
[3] Acetonitrile fact sheet, Australian Government, Department of the Environmental and Water Resources, On-line at: http://www.npi.gov.au/database/substance-info/profiles/4.html.
[4] M.R. Shah, R.D. Noble, D.E. Clough, Pervaporation—air stripping hybrid process for removal of VOCs from groundwater, J. Membr. Sci. 241 (2004) 257–263.
[5] M. Khayet, T. Matsuura, Pervaporation and vacuum membrane distillation processes: modeling and experiments, AIChE J. 51 (2004) 1697–1712.
[6] B. Wu, X. Tan, K. Li, W.K. Teo, Removal of 1,1,1-trichloroethane from water using a polyvinylidene fluoride hollow fiber membrane module: vacuum membrane distillation operation, Sep. Purif. Technol. 52 (2) (2006) 301–309.
[7] Z. Jin, D.L. Yang, S.H. Zhang, X.G. Jian, Removal of 2,4-dichlorophenol from wastewater by vacuum membrane distillation using hydrophobic PPESK hollow fiber, Chinese Chem. Lett. 18 (2007) 1543–1547.
[8] N. Couffin, C. Cabassud, V. Lahoussine-Turcaud, A new process to remove halogenated VOCs for drinking water production: vacuum membrane distillation, Desalination 117 (1998) 233–245.
[9] M. Khayet, T. Matsuura, Surface modification of membranes for the separation of volatile organic compounds from water by pervaporation, Desalination 148 (2002) 31–37.
[10] S. Das, A.K. Banthia, B. Adhikari, Removal of chlorinated volatile organic contaminants from water by pervaporation using a novel polyurethane urea–poly (methyl methacrylate) interpenetrating network membrane, Chem. Eng. Sci. 61 (2006) 6454–6467.
[11] T. Ohshima, Y. Kogami, T. Miyata, T. Uragami, Pervaporation characteristics of cross-linked poly(dimethylsiloxane) membranes for removal of various volatile organic compounds from water, J. Membr. Sci. 260 (2005) 156–163.
[12] Q.L. Liu, J. Xiao, Silicalite-filled poly(siloxane imide) membranes for removal of VOCs from water by pervaporation, J. Membr. Sci. 230 (2004) 121–129.
[13] M. Peng, L.M. Vane, S.X. Liu, Recent advances in VOCs removal from water by pervaporation, J. Hazard. Mater. 98 (2003) 69–90.
[14] L.M. Vane, F.R. Álvarez, Full-scale vibrating pervaporation membrane unit: VOC removal from water and surfactant solutions, J. Membr. Sci. 202 (2002) 177–193.
[15] T. Uragami, H. Yamada, T. Miyata, Removal of dilute volatile organic compounds in water through graft copolymer membranes consisting of poly(alkylmethacrylate) and poly(dimethylsiloxane) by pervaporation and their membrane morphology, J. Membr. Sci. 187 (2001) 255–269.
[16] L. Hitchens, L.M. Vane, F.R. Álvarez, VOC removal from water and surfactant solutions by pervaporation: a pilot study, Sep. Purif. Technol. 24 (2001) 67–84.
[17] S.P. Moulin, Q.T. Nguyen, D. Roizard, P. Aptel, Removal of volatile organic components (VOCs) from water by pervaporation: separation improvement by Dean vortices, J. Membr. Sci. 142 (1998) 129–141.
[18] A. Hasanoglu, Y. Salt, S. Keleser, S. Ozkan, S. Dincer, Pervaporation separation of organics from multicomponent aqueous mixtures, Chem. Eng. Process. 46 (2007) 300–306.
[19] A.M. Urtiaga, E.D. Gorri, G. Ruiz, I. Ortiz, Parallelism and differences of pervaporation and vacuum membrane distillation in the removal of VOCs from aqueous streams, Sep. Purif. Technol. 22–23 (2001) 327–337.
[20] L.Y. Jiang, T.S. Chung, R. Rajagopalan, Dehydration of alcohols by pervaporation through polyimide Matrimid asymmetric hollow fibers with various modifications, Chem. Eng. Sci. 63 (2008) 204–216.
[21] L. Zhang, P.Y. Yunbai Luo, Dehydration of caprolactam–water mixtures through cross-linked PVA composite pervaporation membranes, J. Membr. Sci. 306 (2007) 93–102.
[22] R.S. Veerapur, K.B. Gudasi, T.M. Aminabhavi, Pervaporation dehydration of isopropanol using blend membranes of chitosan and hydroxypropyl cellulose, J. Membr. Sci. 304 (2007) 102–111.
[23] V.V. Namboodiri, L.M. Vane, High permeability membranes for the dehydration of low water content ethanol by pervaporation, J. Membr. Sci. 306 (2007) 209–215.
[24] M. Khayet, M.M. Nasef, J.I. Mengual, Radiation grafted poly(ethylene terephthalate)-graft-polystyrene pervaporation membranes for organic/organic separation, J. Membr. Sci. 263 (2005) 77–95.
[25] B. Smitha, D. Suhanya, S. Sridhar, M. Ramakrishna, Separation of organic–organic mixtures by pervaporation—a review, J. Membr. Sci. 241 (2004) 1–21.
[26] M. Khayet, M.M. Nasef, J.I. Mengual, Application of poly(ethylene terephthalate)-graft-polystyrene membranes in pervaporation, Desalination 193 (2006) 109–118.
[27] M. Khayet, J.P.G. Villaluenga, J.L. Valentin, M.A. López-Manchado, J.I. Mengual, B. Seoane, Filled poly(2,6-dimethyl-1,4-phenylene oxide) dense membranes by silica and silane modified silica nanoparticles: characterization and application in pervaporation, Polymer 46 (2005) 9881–9891.
[28] J.P.G. Villaluenga, M. Khayet, P. Godino, B. Seoane, J.I. Mengual, Analysis of the membrane thickness effect on the pervaporation separation of methanol/methyl tertiary butyl ether mixtures, Sep. Purif. Technol. 47 (2005) 80–87.
[29] M. Khayet, J.P.G. Villaluenga, M.P. Godino, J.I. Mengual, B. Seoane, K.C. Khulbe, T. Matsuura, Preparation and application of dense poly(phenylene oxide) membranes in pervaporation, J. Colloid. Interf. Sci. 278 (2004) 410–422.
[30] J. Antony, Design of Experiments for Engineers and Scientists, Butterworth-Heinemann, Oxford, 2003.
[31] D.C. Montgomery, Design and Analysis of Experiments, 5th ed., John Wiley & Sons, New York, 2001.
[32] M. Khayet, C. Cojocaru, M.C. García-Payo, Application of response surface methodology and experimental design in direct contact membrane distillation, Ind. Eng. Chem. Res. 46 (2007) 5673–5685.
[33] C. Cojocaru, G. Zakrzewska-Trznadel, Response surface modeling and optimization of copper removal from aqua solutions using polymer assisted ultrafiltration, J. Membr. Sci. 298 (2007) 56–70.
[34] F. Xiangli, W. Wei, Y. Chen, W. Jin, N. Xu, Optimization of preparation conditions for polydimethylsiloxane (PDMS)/ceramic composite pervaporation membranes using response surface methodology, J. Membr. Sci. 311 (2008) 23–33.
[35] M. Khayet, C. Cojocaru, G. Zakrzewska-Trznadel, Response surface modeling and optimization in pervaporation, J. Membr. Sci. 321 (2008) 272–283.
[36] M. Khayet, C. Cojocaru, G. Zakrzewska-Trznadel, Studies on pervaporation separation of acetone, acetonitrile and ethanol from aqueous solutions, Sep. Purif. Technol. 63 (2008) 303–310.
[37] S. Akhnazarova, V. Kafarov, Experiment optimization in chemistry and chemical engineering, Mir Publisher, Moscow, 1982.
[38] M. Redhe, M. Giger, L. Nilson, An investigation of structural optimization in crashworthiness design using stochastic approach, Struct. Multidisc. Optim. 27 (2004) 446–459.
[39] M. Tomescu, A.I. Maniu, S. Cretu, G. Rachiteanu, Application of statistical mathematical methods for conducting of chemical processes (in Romanian), Rev. Chim. (Bucharest) 35 (11) (1984) 1012–1017.
[40] G. Derringer, R. Suich, Simultaneous optimization of several response variables, J. Qual. Technol. 12 (1980) 214–221.
[41] K.L. Hsieh, L.I. Tong, H.P. Chiu, H.Y. Yeh, Optimization of a multi-response problem in Taguchi's dynamic system, Comput. Ind. Eng. 49 (2005) 556–571.
[42] I.J. Jeong, K.J. Kim, D-STEM: a modified step method with desirability function concept, Comput. Oper. Res. 32 (2005) 3175–3190.
[43] S.H.R. Pasandideh, S.T.A. Niaki, Multi-response optimization using genetic algorithm within desirability function framework, Appl. Math. Comput. 175 (2006) 366–382.